Probabilistic Creep Modeling of 304 Stainless Steel Using a Modified Wilshire Creep-Damage Model

Conference Paper · November 2020

DOI: 10.1115/PVP2020-21613

3 authors, including:

Md Abir Hossain
University of Texas at El Paso
5 PUBLICATIONS **4** CITATIONS
SEE PROFILE

Jaime Cano
University of Texas at El Paso
4 PUBLICATIONS **3** CITATIONS
SEE PROFILE

Proceedings of the ASME 2020
Pressure Vessels & Piping Conference
PVP2020
August 3, 2020, Virtual, Online

PVP2020-21613

PROBABILISTIC CREEP MODELING OF 304 STAINLESS STEEL USING A MODIFIED WILSHIRE CREEP-DAMAGE MODEL

Md Abir Hossain, Jaime A. Cano, and Calvin M. Stewart
Department of Mechanical Engineering
The University of Texas at El Paso
El Paso, TX

ABSTRACT

Pressure vessel components subject to high temperature and pressure are susceptible to life-limiting creep and/or creep-induced failure. Traditional continuum damage mechanics (CDM) based creep-damage model are used extensively for the prediction and design against creep in these components. Conventional creep experiments show considerable uncertainty in the creep response of materials where scatter can span decades of creep life. The objective of this paper is to introduce the probabilistic methods into a deterministic creep-damage model in order to predict experimental uncertainty. In this study, a modified Wilshire model capable of creep deformation, damage, and rupture prediction is selected. Creep deformation data for 304 stainless steel is collected from the literature consisting of quintuplicate (five) tests at 600°C with varying stress levels. It is hypothesized that the scatter in creep data is due to: test condition (temperature fluctuations and eccentric loading), initial damage (pre-existing surface and sub-surface defects), and metallurgical (local variation in microstructure) uncertainties. Probability distribution functions (pdfs) and Monte Carlo simulations are applied to introduce the uncertainties into the modified Wilshire equations. The domain of each source of uncertainty must be defined. A systematic calibration approach is followed where the material constant for each creep curve (in the quintuple) are obtained and statistical analysis is performed on the material properties to assess the random distribution associated with each uncertain material parameter. The probabilistic calibration begins with the introduction of test condition randomness (±2°C and ±3.2% MPa of nominal temperature/stress) in accordance with the ASTM standards. Cross calibration of temperature-stress variability proceeds the approximation of initial damage uncertainty which captures the remaining scatter in the data. Deterministic calibration unveils the range of variabilities associated with the material properties. The best-fitted pdfs are assigned to each uncertain parameter and subsequently, the deterministic model is converted into a probabilistic model where reliability is a tunable factor. A large number of Monte Carlo simulation are conducted to generate probabilistic creep deformation, minimum-creep-strain-rate (MCSR), and stress-rupture (SR) predictions. It is demonstrated that the probabilistic model produces quantitatively and qualitatively good fits when compared with experimental data. Future work will be directed towards the inclusion of service condition related uncertainty (power plant, turbine blade, Gen IV nuclear reactor application) into the probabilistic framework where the uncertainties are more robust.

Keywords: Creep; Life prediction; Monte Carlo method; Probabilistic; Reliability; Uncertainty.

NOMENCLATURE

$\dot{\varepsilon}_{\min}$	minimum-creep-strain-rate
ε_{pr}	primary creep strain
A	Creep Coefficient
σ_s	Secondary Creep mechanism-transition stress
M, σ_t, χ	Sinh model material constant
k_1, u, k_2, v	Wilshire model material constant
CSR	creep-strain-rate
CDM	continuum damage mechanics
FCSR	final-creep-strain-rate
MCSR	minimum-creep-strain-rate
MC	Monte Carlo simulation
pdf(s)	probability distribution function(s)
SR	stress-rupture
WCS	modified Wilshire model

1. INTRODUCTION

1.1 Motivation

Creep deformation and failure is a stress, temperature, and time dependent phenomenon that reveals remarkable scattering. With the given uncertainty of creep and the understanding that

long-term creep data (when temperatures are high and stresses are low) can exhibit scatter across decades (log scale); it is difficult to elucidate the service life of a long-lived component without an inflated safety factor and operational compromise. Rather than taking a deterministic approach and calibrate predictive models to the average-line in the scattered data, the uncertainty in the creep data must be integrated into the probabilistic modeling approach. The origin of the uncertainty in the data stems from many sources; notably, service temperature and pressure oscillation, surface and subsurface defects, metallurgical inhomogeneity, thermomechanical history due to processing or prior service that influence bulk properties, geometric parameters, and test procedure (operator and machine) error [1-5]. The incorporation of all these sources of uncertainty into creep deformation, damage, and rupture predictions poses a challenge. The mutual interaction and interference among the sources of uncertainty potentially could lead to unrealistic scatter in creep data. Care must be taken when incorporating competing sources of uncertainty in a probabilistic model to avoid over-exaggerated predictions. The calibration of a probabilistic model starts with the selection and validation of a creep-damage model from a deterministic standpoint.

1.2 Uncertainty in Creep-Rupture Data

By their very nature, experimental creep deformation data take a long time to accumulate and there is usually a remarkable amount of scattering in the data. For steels, within the specified composition limits, the creep rupture properties show considerable batch to batch scatter. There are a number of sources of uncertainty that are causing this scattering in the creep deformation data. These and other uncertainties have justified the completion of many long-term test programs for many different power plant steels involving multiple batches of various product forms, e.g. tube, pipe, plate, and forgings. Previous studies revealed the presence of non-negligible yet significant scattering in the creep deformation and rupture data [6-13]. Studies of Rutmen et al. reported the aggregated creep rupture data variation by an order of magnitude for two different high temperature alloy [6]. Creep rupture tests on 316 stainless steel by Garofalo et al. revealed the rupture variation by a factor of 4.5 [7]. Penny et al. noticed the scattering of rupture time in order of 10 hours in the replicated creep rupture experiments [8]. Hayhurst directed his research towards explaining the effects of test variables on the scatter in creep data and revealed a small fluctuation of temperature ±3°C can lead to ±8% variation in creep rupture [9]. It was also reported that loading eccentricity of 1.5% can reduces the rupture life by up to 60%. Farris et al. showed experimental evidence for load eccentricity with creep rupture tests of copper-bicrystal exhibiting 60% life reduction due to 2-12% eccentric loading [10]. Kim et al. performed the short-term creep test on 304 Stainless Steel and found that Coefficient of variation (%CoV) of initial strain, minimum-creep-strain-rate, and creep ductility are two to three times higher than creep rupture [11]. Evans et al. statistically analyzed the creep rupture data of 0.25Cr-0.5Mo-0.25V and observed the scattering of failure time by a factor of 6-7 [12]. In a separate study by Booker et al. conducted on creep rupture properties of 2.25Cr-1Mo steel of 53 different heats of materials and concluded that average rupture time for single-heat vary over staggering range of 4000 to 100000 hours [13]. These wide ranges of scattering in creep deformation to rupture data spanning decades make the accurate lifetime estimation a cumbersome and crude procedure.

To that end, many novel approaches are adopted for safe and durable lifetime prediction based on the deterministic creep laws. Past methods such as Larson-Miller method, Manson Hafred method, and a range of other techniques have proved notoriously inconsistent in a predictive capacity [14-15]. Demonstration of the difficulties associated with these techniques are wide ranging. A number of modern approaches have been developed in recent years which have sought to address the issue with varying degree of success [16-19]. To that end, the Wilshire equations were first proposed in 2007 by Wilshire and Battenbough in the pursuit of more physically relevant representations of creep data predictions [20]. The Wilshire equations have been calibrated to polycrystalline copper, 11Cr-2W (Grade 122) and 9-12% chromium steel, 1Cr-1Mo-0.25V, 316H stainless steel, 12Cr stainless steel bars of turbine blades [21-23]. The Wilshire equations have also been validated in the capability to make predictions for a single material in multiple forms (plate, tube, and pipe) [24]. From an analytical standpoint, the Wilshire model's ability to predict the creep deformation (via time-to-creep-strain predictions) is complex and exhibits a crude calibration approach. The equations' lack of a closed-form solution and incompatibility in finite element analysis has led to the development of the modified Wilshire model presented in this paper.

1.3 Wilshire Model

The Wilshire equations for stress-rupture (SR), t_r and minimum-creep-strain-rate (MCSR), $\dot{\varepsilon}_{\min}$ prediction are

$$\frac{\sigma}{\sigma_{TS}} = \exp\left(-k_1\left[t_r \exp\left(-\frac{Q_c^*}{RT}\right)\right]^u\right) \quad (1)$$

$$\frac{\sigma}{\sigma_{TS}} = \exp\left(-k_2\left[\dot{\varepsilon}_{\min} \exp\left(\frac{Q_c^*}{RT}\right)\right]^v\right) \quad (2)$$

Where Q_c^* (Jmol^{-1}) is the creep activation energy, R is the universal gas constant (8.314 Jmol^{-1}K^{-1}), T is the temperature in Kelvin, σ (MPa) is the applied stress, σ_{TS} (MPa) is the tensile strength, and k_1 (in hr^{-u}), u, k_2 (in hr^{v}), and v are material constants [20-22]. The Wilshire calibration process is analytical. Creep activation energy, Q_c^* is obtained by plotting the experimental $\ln(\dot{\varepsilon}_{\min})$ or $\ln(t_r)$ versus $1/T$ for a fixed stress ratio, σ/σ_{TS} and taking the slope. The material constants k_1 and u are determined by plotting the experimental $\ln\left[-\ln(\sigma/\sigma_{TS})\right]$

versus $\ln\left[t_r \exp\left(-Q_c^*/RT\right)\right]$ in which the slope is u and the y-intercept is the k_1 constant. Similarly, k_2 and v are obtained by plotting the experimental $\ln\left[-\ln(\sigma/\sigma_{TS})\right]$ versus $\ln\left[\dot{\varepsilon}_{\min} \exp\left(Q_c^*/RT\right)\right]$ where the slope is v and the y-intercept is the k_2 constant. Rupture and MCSR predictions are made by rearranging [Eq. (1)] and [Eq. (2)] as follows

$$t_r = \frac{\left[-\ln\left(\frac{\sigma}{\sigma_{TS}}\right)\Big/k_1\right]^{\frac{1}{u}}}{\exp\left(-Q_c^*/RT\right)} \tag{3}$$

$$\dot{\varepsilon}_{\min} = \frac{\left[-\ln\left(\frac{\sigma}{\sigma_{TS}}\right)\Big/k_2\right]^{\frac{1}{v}}}{\exp\left(Q_c^*/RT\right)} \tag{4}$$

to obtained desired t_r and $\dot{\varepsilon}_{\min}$ at given stress and temperature. The Wilshire equations has shown credible extrapolations across multi-batch short-term stress-rupture data, typically less than 5000 hours, out to 100,000 hours for multiple isotherms [25-26]. When properly calibrated, the Wilshire equations predict the SR and MCSR over a wide range of temperature and stress [27].

A third time-to-creep-strain equation exists that can be used to make predictions of time-to-creep-strain and rearranged to make predictions of creep deformation to rupture.

$$\frac{\sigma}{\sigma_{TS}} = \exp\left(-k_3\left[t_\varepsilon \exp\left(-\frac{Q_c^*}{RT}\right)\right]^w\right) \tag{5}$$

where k_3 and w are material constants at a constant creep strain, ε_{cr} [21,25]. Harrison assessed the time-to-strain approach to predict the creep deformation prediction for alloy 720Li [28]. Evans studied the time-to-strain approach in Waspaloy [29]. However, the result obtained showed over-prediction in the time for failure as well as in the creep strain curves [28-29]. There seems to be a variety of complications in using the time-to-strain equation to predict creep deformation and little inconsistency on the methods of implementation.

1.4 Sine-Hyperbolic (Sinh) Model

The continuum damage mechanics (CDM) based Sine-hyperbolic (Sinh) model was developed to model the secondary and tertiary creep regimes of metallic materials [30]. The Sinh model consists of coupled creep-strain-rate (CSR) and damage evolution equations as follows

$$\dot{\varepsilon}_{cr} = A\sinh\left(\frac{\sigma}{\sigma_s}\right)\exp(\lambda\omega) \tag{6}$$

$$\dot{\omega} = \frac{\left[1-\exp(-\phi)\right]}{\phi} M \sinh\left(\frac{\sigma}{\sigma_t}\right)^{\chi} \exp(\phi\omega) \tag{7}$$

where A is the creep coefficient, σ_s is secondary creep mechanism-transition stress, M, σ_t, and χ are material constants that must be greater than zero, σ is stress, and ω is damage an internal state variable that evolves from an initial damage to unity. Note, [Eq. (6)] is a modified form of the Sinh CSR to enable a closed-form creep strain equation [31].

Assume that initial damage is zero, $\omega_o = 0$. The secondary creep material constants A and σ_s can be calibrated as

$$\dot{\varepsilon}_{\min} = A\sinh\left(\frac{\sigma}{\sigma_s}\right) \tag{8}$$

where $\dot{\varepsilon}_{\min}$ is the minimum-creep-strain-rate (MCSR) measured from creep data. The constant λ is unit-less and equal to

$$\lambda = \ln\left(\frac{\dot{\varepsilon}_{\text{final}}}{\dot{\varepsilon}_{\min}}\right) \tag{9}$$

where $\dot{\varepsilon}_{\text{final}}$ is the final-creep-strain-rate (FCSR) measured from creep data. The λ constant exhibits stress and/or temperature dependence. Integration furnishes damage, ω and rupture, t_r predictions

$$\omega(t) = -\frac{1}{\phi}\ln\left[1-\left[1-\exp(-\phi)\right]\frac{t}{t_r}\right] \tag{10}$$

$$t_r = \left[M \sinh\left(\frac{\sigma}{\sigma_t}\right)^{\chi}\right]^{-1} \tag{11}$$

where initial time, t_o is set to zero. Damage [Eq. (10)] depends on the ϕ material constant and rupture predictions [Eq. (11)]. The ϕ constant controls the damage trajectory and is stress and/or temperature dependent. The rupture prediction [Eq. (11)] depends on the M, σ_t, and χ material constants. The material constant σ_t facilitates the transition from the low-stress to high-stress regime.

Assuming that initial damage in non-zero, $\omega_o > 0$ (i.e. the material has pre-existing sub-surface defects), integration of [Eq. (7)] reduces the damage prediction into the following form.

$$\omega(t) = -\frac{1}{\phi}\ln\left[\exp(-\phi\omega_o) - \left[\exp(-\phi\omega_o) - \exp(-\phi)\right]\frac{t}{t_r}\right] \tag{12}$$

where initial damage, $\omega_o > 0$ cause the initial CSR [Eq. (6)] and damage rate [Eq. (7)] to increase while decreasing the remaining life to rupture.

The separable MCSR and rupture [Eqs. (8) & (11)] laws in the Sinh model allow the Wilshire and Sinh modes to be combined to the modified Wilshire model presented in this paper.

2. RESEARCH OBJECTIVE

The aim of this study is to develop a probabilistic modified Wilshire (WCS) model for long-term creep defamation, damage, and rupture prediction that incorporates multi-sources of

uncertainty. The objective of this study includes a robust methodological scheme to determine how various sources of uncertainty interact to contribute to the overall creep resistance of a material. To attain the research objectives the following steps are undertaken.

- The modified Wilshire model is introduced.
- Replicant creep deformation data of type 304 stainless steel is gathered from literature [11].
- Intrinsic uncertainties of the data are assessed, and model constants are calibrated (Wilshire and Sinh) to examine the associated variabilities.
- Temperature and stress fluctuation are introduced into the probabilistic assessment according to ASTM E139 and ASTM E8 standards respectively [34-35].
- Each uncertain parameter is assigned a probability distribution functions (pdf) according to associated variability of the parameter. Probabilistic predictions are performed to demonstrate the interference and/or enhancement of uncertainty due to interaction of multi-sources of uncertainty.
- A large number of Monte Carlo simulated creep deformation curves verify the reliability and accuracy of the WCS creep-damage model.
- The extrapolated MCSR and SR bands prove the conservatism of the WCS model from a probabilistic standpoint.

3. MODIFIED WILSHIRE (WCS) MODEL

The novel CDM-based modified Wilshire model consists of coupled creep-strain-rate (CSR) and damage evolution equations. For brevity, the model is referred to as the WCS model. The CSR equation is furnished by taking the Sinh CSR [Eq. (6)] and replacing the Sinh MCSR [Eq. (8)] with Wilshire's MCSR [Eq. (4)] as follows

$$\dot{\varepsilon}_{cr} = \frac{\left[-\ln\left(\frac{\sigma}{\sigma_{TS}}\right)\Big/k_2\right]^{\frac{1}{v}}}{\exp\left(Q_c^*/RT\right)}\exp(\lambda\omega) \tag{13}$$

The damage evolution is furnished by taking the Sinh damage evolution [Eq. (7)] and replacing the Sinh rupture prediction [Eq. (11)] with Wilshire's rupture prediction [Eq. (3)] as follows

$$\dot{\omega} = \frac{\left[1-\exp(-\phi)\right]}{\phi}\frac{\exp\left(-Q_c^*/RT\right)}{\left[-\ln\left(\frac{\sigma}{\sigma_{TS}}\right)\Big/k_1\right]^{\frac{1}{u}}}\exp(\phi\omega) \tag{14}$$

The internal state variable damage, ω from Sinh is preserved [Eq. (10)]. The complete WCS model is summarized in Table 1. The Wilshire material constants $\left(Q_c^*, k_1, u, k_2, v\right)$ and Sinh material constants (λ, ϕ) can be determined using the existing calibration approach for each model respectively [21-24,30-33]. Any Wilshire or Sinh constants that have been previously calibrated for a given material can be directly applied in the new model.

Table 1 :Summary of the WCS model

Feature	Equation	Origin	Material Constants
MCSR	[Eq. (4)]	Wilshire	Q_c^*, k_2, v
Rupture	[Eq. (3)]	Wilshire	Q_c^*, k_1, u
CSR	[Eq. (13)]	Combined	Q_c^*, k_2, v, λ
Damage Rate	[Eq. (14)]	Combined	Q_c^*, k_1, u, ϕ
Damage	[Eq. (12)]	Sinh	ϕ

4. MATERIALS: 304 STAINLESS STEEL

Alloy 304 stainless steel (304SS) is a widely used Fe-Cr-Ni alloy. Creep deformation data for 304SS bar was gathered from literature [11]. The chemical composition (wt %) of the alloy 304 SS is listed in Table 2. The tensile strength, yield strength, elongation is 706 MPa, 490 MPa, and 18% at room temperature respectively. The tensile strength, σ_{TS} of 304 stainless steel at 600°C is approximately 386 MPa. A total of ten creep curves where collected with five replicate tests at 300 and 320 MPa subject to 600°C. The creep specimens were fabricated from 20 mm diameter according to ASTM E139 standard [34]. The creep tests were carried out following the ASTM E139 standard [34].

Table 2 : Chemical composition of 304SS bar in wt% [11]

Element	wt%
C	0.02
Si	0.40
Mn	1.83
P	0.029
S	0.009
Ni	8.13
Cr	18.22
Mo	0.24
Cu	2.06
N	0.102

5. RESULTS AND DISCUSSION

5.1 Calibration of Material Constants

At first, the novel WCS model is calibrated deterministically to assess the accuracy of the model prediction. To that end, the material constants of Wilshire and Sinh are calibrated according to the existing calibration approaches discussed in sections 1.3 and 1.4 respectively. The activation energy, Q_c^* is found to be 118 KJmol^{-1}.

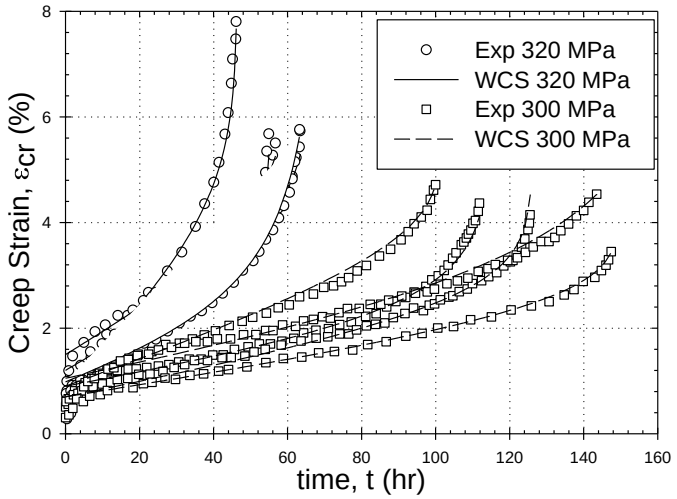

Figure 1: Deterministic creep deformation predictions using the WCS model for 304SS at 300 and 320 MPa and 600°C

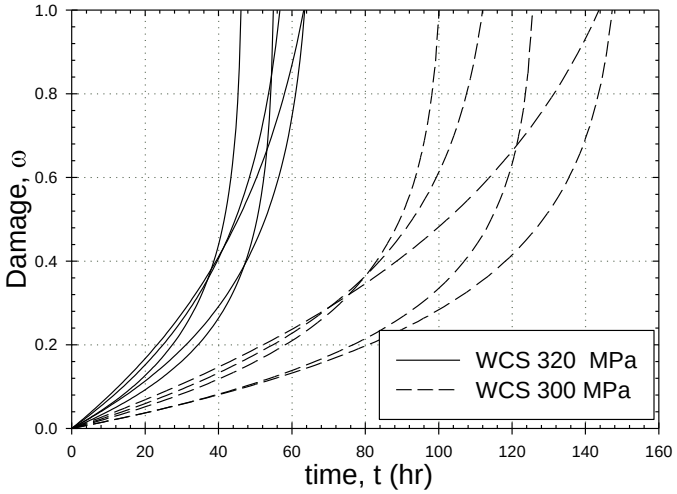

Figure 2: Deterministic damage predictions using the WCS model for 304SS at 300 and 320 MPa and 600°C

The 5 replicant tests at each stress level (320 and 300 MPa), result in 5 set of Wilshire constants (k_1, u, k_2, v). The Sinh constant λ and ϕ is calculated and optimized per test respectively. The primary creep strain rate, ε_{pr} is measured per test. Subsequently, a set of 10 Sinh material constants $(\lambda, \phi, \varepsilon_{pr})$ are obtained.

Creep deformation predictions of the WCS model using the calibrated material constants are shown in Figure 1. Qualitatively, the calibrated material constants produce high quality fits to the experimental data. Quantitatively, the coefficient of variation (%CoV) in creep ductility is 0.52% for 320 MPa and 7.70% for 300 MPa respectively. For creep rupture, the coefficient of variation (%CoV) is low at 1.18% for 320 MPa and 1.23% for 300 MPa. The CDM-based WCS model also exhibits the ability to predict the damage evolution from zero as shown in Figure 2. In all cases, the damage is equal to unity at rupture and the damage rates remain finite at rupture.

5.2 Probabilistic Model

The probabilistic model is developed by analyzing the sources of uncertainties and their relative distribution. The probabilistic model takes two kinds of input: fixed and uncertain. The fixed parameters are the activation energy, Q_c^* and tensile strength, σ_{TS}. The uncertain parameters are: test conditions $(T$ and $\sigma)$, the material constants [Wilshire (k_1, u, k_2, v) and Sinh (λ, ϕ)], and initial damage, ω_o. The sources of uncertainties are material/test dependent and do not exhibit any time-dependency.

5.3 Probabilistic Calibration

Probability distribution functions are calibrated for test conditions, material constants, and initial damage in this section.

The uncertainty of test conditions is adopted based on the ASTM standards. The ASTM E139 standard states that temperature during testing must not fluctuate more than ±2°C below 1000°C and ±3°C above 1000°C [34]. The specimens in this study are subject to temperatures below 1000°C so a variation of ±2°C is applied. The ASTM E8 standard finds the stress increases of 1.5, 2.5, and 3.2% for 12, 5, 9, and 6 mm diameter specimens respectively when load eccentricity is 0.025 mm [35]. The eccentricity matches the typical dimensional tolerances in specimens. The specimen is this study have a 6 mm diameter so a variation of 3.2% stress variation is applied. Normal Gaussian pdfs are assigned to temperature and stress variations. In this case, neither temperature nor stress has enough experimental data to calibrate credible Normal Gaussian distribution; so, to avoid exaggerated and sub-standard predictions the mean is set to the nominal temperature/stress and the standard deviation is set to 1/8th of the range. Test condition uncertainty is applied based on the ASTM standards rather than the actual laboratory data. Additionally, this study has been developed employing the worst-case scenario at a laboratory setup with the aim of extending this study at an industrial setup where the operating condition uncertainty is even more crude. In reality, the test condition uncertainty recorded in the laboratory while conducting a creep test is much lower than the ASTM standard. However, this accuracy depends on the quality of machine used (heating chamber), thermocouple quality, eccentric loading, and the operator errors.

The Wilshire material constants $(k_1, u$ and $k_2, v)$ are modeled as a Normal Gaussian distribution. The 5 sets of Wilshire material constants are not enough to model a credible Normal Gaussian pdf and produce a realistic tail distribution; so, the Wilshire constants are modeled setting the mean equal to the mean of the calibrated values and standard deviation as 1/8th of the range.

The uncertainty of the Sinh material constant $(\lambda$ and $\phi)$ is modeled based on the deterministically calibrated values. Both

the material constant $(\lambda$ and $\phi)$ show temperature and stress dependence. This temperature-stress dependency is modeled using Eyring's equation. The material constant, λ is modeled as follows

$$\lambda(T,\sigma) = \lambda_o \exp\left(-\frac{V_\lambda^* \sigma}{k_b T}\right) \qquad (15)$$

$$\lambda \geq 0$$

where λ_o is a unitless coefficient, V_λ^* is the activation energy in $\left(\text{cm}^3\right)$, σ is stress in (MPa), T is temperature in (K), and k_b is the Boltzmann constant 1.3806×10^{-23} in (J/K). Due to the nature of distribution of the calibrated λ constants, the uncertainty of λ is set by a 2-parameter Weibull distribution. The overall uncertainty of λ is driven by the uncertainty of λ_o, uncertainty of set temperature and stress, and by setting the activation volume, V_λ^* equal to 3.39×10^{-23} cm^3.

The material constant, ϕ is modeled as follows

$$\phi(T,\sigma) = \phi_o \exp\left(\frac{V_\phi^* \sigma}{k_b T}\right) \qquad (16)$$

$$\phi \geq 1$$

where ϕ_o is a unitless coefficient, V_ϕ^* is the activation energy in $\left(\text{cm}^3\right)$, σ is stress in (MPa), T is temperature in (K), and k_b is the Boltzmann constant 1.3806×10^{-23} in (J/K). Due to skewed nature of the calibrated ϕ constants, the uncertainty of ϕ is modeled using 2-parameter Weibull distribution. The overall uncertainty of ϕ is established by the variation of ϕ_o, uncertainty of set temperature and stress, and by setting the activation volume, V_ϕ^* equals 2.79×10^{23} cm^3.

The uncertainty of primary creep strain, ε_{pr} is established by measurement. The ε_{pr} does not show temperature and/or stress dependency. The ε_{pr} is assigned a Normal Gaussian pdf with the mean and standard deviation set to 0.785 and 0.307 respectively. The distribution of ε_{pr} is set by (mean ±2 x standard deviation) of a Normal Gaussian pdf.

The initial and pre-existing defect is an intrinsic phenomenon assumed to be varied specimen-to-specimen. It is hypothesized that bulk of the test-specimens are not affected by the pre-existing surface and sub-surface defects, so the initial damage, ω_o uncertainty is modeled by the exponential distribution. Setting the worst-case scenario for temperature and stress $(T+2°\text{C}$ and $\sigma+3.2\%$ MPa$)$, and setting the calibrated material constants to maximum value, the limits of the range of initial damage, ω_o carried by the specimens are calibrated. The estimated initial damage, ω_o carry the remaining uncertainty in the data after applying the worst-case scenario into the experimental data.

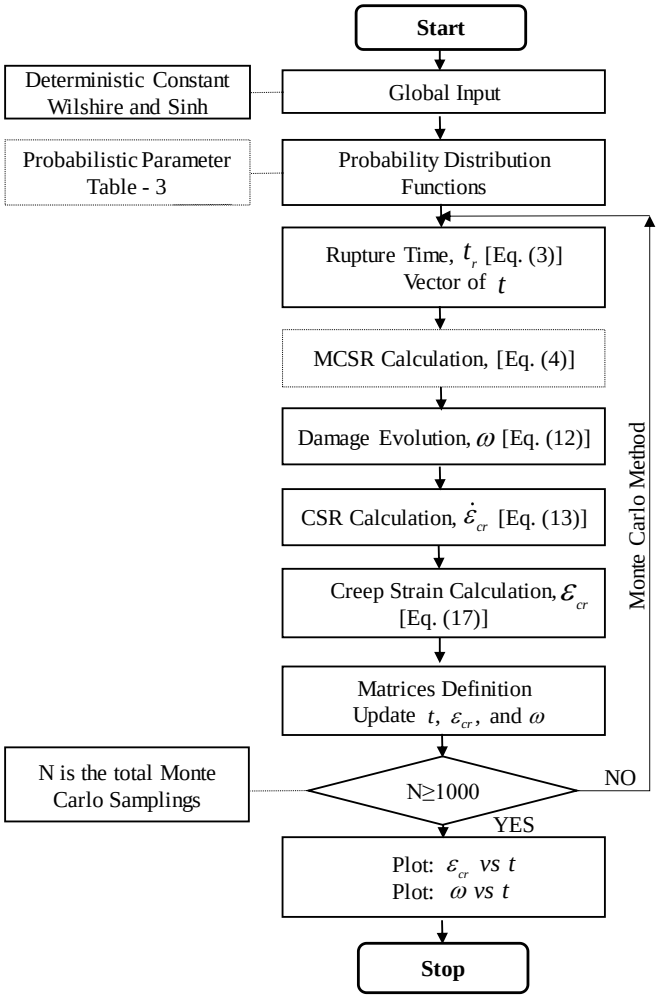

Figure 3: Flowchart of Monte Carlo method for probabilistic prediction by WCS model.

The uncertain parameter discussed above and the associated pdfs employed in the probabilistic model are reported in Table 3.

5.4 Probabilistic Creep Deformation Prediction

For probabilistic creep deformation and rupture prediction, a subroutine in MATLAB was developed. The flowchart of the Monte carlo method for probabilistic assessment is illustrated in Figure 3. The subroutine takes the probabilistic input parameter as reported in Table 3 and performs Monte Carlo simulation is to generate probabilistic predictions. The probabilistic rupture time, t_r is calibrated by using [Eq. (3)] and converted into a vector of time, t. The damage evolution is calibrated using the initial damage form of Sinh [Eq. (12)] in conjunction with time

Table 3 : Probability distributions functions (pdfs) for each uncertain parameter in the WCS model.

Parameter	Distribution Shape	Distribution Parameters	Mode of Variation
T	Normal Gaussian	$\mu = X$ ° C | $\sigma = 4$°C/8	Experimental Variation
σ	Normal Gaussian	$\mu = X$ MPa | $\sigma = X \times (6.4\%/8)$ MPa	
u	Normal Gaussian	$\mu = 0.377$ | $\sigma = 0.0343/8$	Model Variation (Wilshire and Sinh)
k_1	Normal Gaussian	$\mu = 20.474$ | $\sigma = 10.326/8$	
v	Normal Gaussian	$\mu = -0.272$ | $\sigma = 0.303/8$	
k_2	Normal Gaussian	$\mu = 7.605$ | $\sigma = 1.789/8$	
ε_{pr}	Normal Gaussian	$\mu = 0.785$ | $\sigma = 0.307$	
λ_o	2-parameter Weibull	$a = 1.814$ | $b = 2.557$	
ϕ_o	2-parameter Weibull	$a = 6.370$ | $b = 2.994$	
ω_o	Exponential	$\mu = 0.005$	Inherent specimen-to-specimen Variation

X is the nominal temperature/stress of interest.

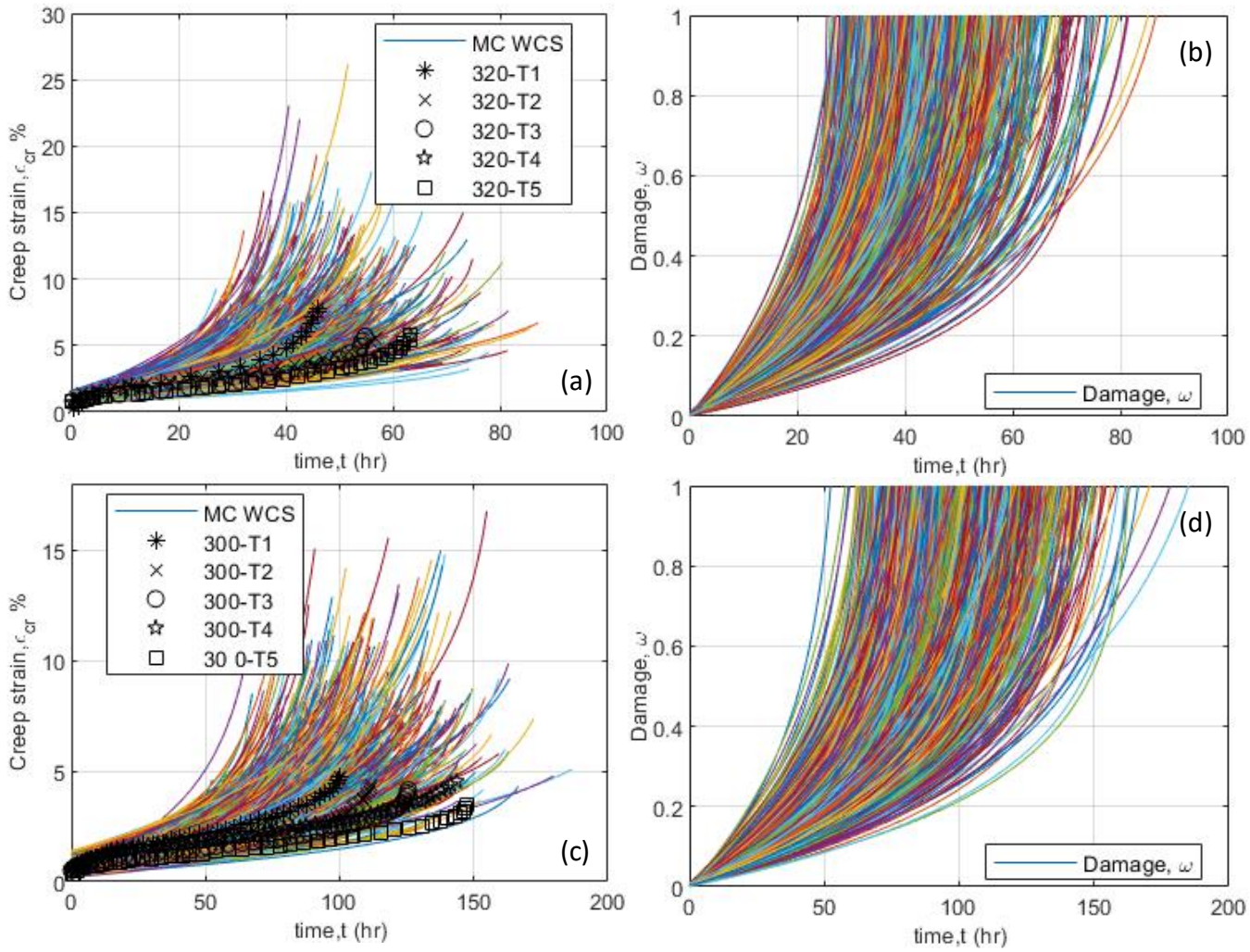

Figure 4: Probabilistic creep deformation and damage predictions for 304SS at (a-b) 320 MPa and (c-d) 300 MPa and 600°C

vector, t to predict the damage curve at each time step. The CSR equation [Eq. (13)] of WCS model is employed where the current damage is used to calculate creep-strain-rate at each time step. Creep strain is calculated using finite difference method

$$\varepsilon_{cr,i} = \dot{\varepsilon}_{cr,i} \cdot \Delta t + \varepsilon_{cr,i-1} \tag{17}$$

where, $\varepsilon_{cr,i}$ is the creep strain at the current time step and $\varepsilon_{cr,i-1}$ is the creep strain of the previous time step. In this study, the time stepping, $\Delta t = 1$ hr. For each simulation, a unique set of parameters is sampled from the pdfs and feed into the model. A total of 1000 Monte Carlo simulations are performed and hence 1000 unique creep deformation and damage evolution curves are generated for each test conditions.

The full interaction of multi-sources of uncertainty into the probabilistic WCS model for predicting the creep deformation curves at 600°C subjected to 320 and 300 MPa are shown in Figure 4(a) and Figure 4(c) respectively. Qualitatively, the probabilistic creep deformation curves track well with the experimental data. The predictions tend on the conservative side with the outliers representing the worst-case interaction among the sources of uncertainty. The simulated WCS model show 10% and 25% higher creep ductility than the experimental data at 320 and 300 MPa respectively. The co-efficient of variation (%CoV) of WCS model prediction of final creep strain is 29% and 33% higher than experimental data. On the other hand, simulated WCS model show 24% and 23% less rupture prediction than the experimental data at 320 and 300 MPa respectively. The co-efficient of variation (%CoV) of WCS rupture prediction is 10% and 5% higher than experiment. This statistic proves that WCS model final creep strain prediction are more scatter than the rupture prediction. This reveals that the MCSR material constants are more sensitive than SR material constants to the overall creep ductility. A small variation in the MCSR material constants lead to a wide-ranging variation in creep ductility. Careful tuning of MCSR related material constants is needed for more robust probabilistic assessment. A statistical comparison of creep ductility and rupture prediction between the WCS and experimental data are reported in Table 4. The damage evolves from the initial damage, ω_o to unity at rupture at 320 and 300 MPa as shown in Figure 4(b) and Figure 4(d) respectively. In this study, the worst-case scenario at a laboratory test setup is adopted.

Table 4 : Statistical comparison of creep ductility and rupture prediction between WCS model and experimental data.

Stress, σ (MPa)	Type	Creep Ductility* ε_{cr} (%)	Rupture time* t_r (hr)
320	WCS	6.77 | 45%	45.74 | 23%
	Exp	6.09 | 16%	56.83 | 13%
300	WCS	5.62 | 45%	102.41 | 21%
	Exp	4.24 | 12%	125.66 | 16%

* Average | %CoV

However, in an industrial setup, the probabilistic problems are cruder as service condition fluctuation are more severe. Despite the fact of applying multi-faceted random parameters into the model, the probabilistic WCS model depicts a conservative creep deformation behavior, eliminating over-conservatism and/or inadvertent non-conservatism of the approach.

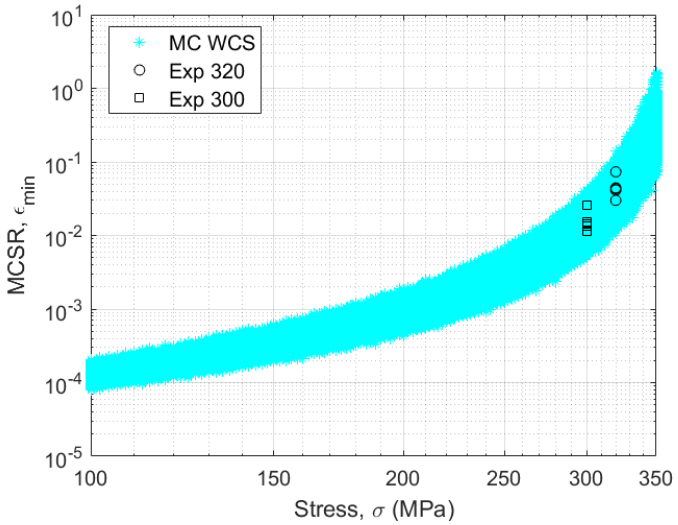

Figure 5: Probabilistic minimum-creep-strain-rate (MCSR) predictions using the WCS model

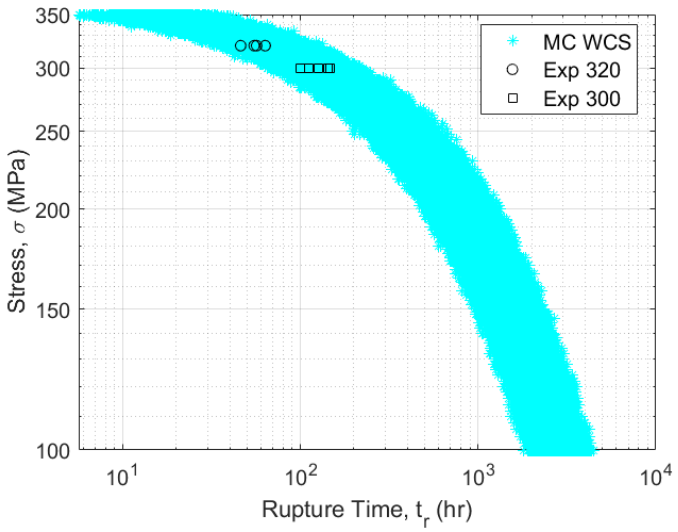

Figure 6: Probabilistic stress-rupture (SR) predictions using the WCS model

5.5 Probabilistic MCSR and SR Prediction

Probabilistic MCSR and SR predictions at 600°C are shown in Figure 5 and Figure 6 respectively. At each stress level, 1000 Monte Carlo simulations were performed. Qualitatively, the MCSR and SR bands show a satisfactory fit to the experimental data. When the short-term data are extrapolated at high temperature and low stress, the scatter bands are conservative. The scatter band expand in the low stress regime matching the

expected creep-rupture behavior. From the standpoint of material design and quantification, the scatter bands represent the safe and reliable design zone and indicative of the under- or over-estimation design point. However, different micro-structural damage mechanism kicks in into the material at high temperature such as grain boundary sliding, factors affecting creep cavitation, growth of nucleation, etc. The variations in such damage phenomena might lead to a wide-ranging deviation in the creep resistance of the material. To effectively quantify and incorporate such micro- and meso-scale damages into the phenomenological models such as CDM-based WCS model poses a challenge both analytically and numerically. These reduced yet substantially significant source of uncertainty should improve the credibility of the overall probabilistic framework. Nonetheless, incorporation of such uncertain sources renders the model both numerically and computationally quite intensive. Future investigation will be conducted on inclusion of different micro- and meso-scale random factors affecting overall creep resistance of the material into probabilistic WCS model without the loss of generality and computational cost.

6. CONCLUSION

Power plant and pressure vessels components are expected to operate closer to their maximum efficiency with a high degree of reliability and durability. However, these long duration service at high temperature-stress regime made the components susceptible to creep and creep induced failure. Lack of complete understanding of such failure necessitate recurring inspections and needless early retirement of components. For reliable and accurate predictions of creep deformation to rupture a robust probabilistic assessment must be adopted. In this study, a CDM-based WCS model is carefully tuned to generate probabilistic prediction without the loss of fidelity and accuracy of the prediction. The probabilistic investigation described in this paper led to following observations.

- The CDM-based WCS model shows a remarkable ability to predict creep deformation to rupture in a deterministic capacity. The WCS model serves as a good platform to initiate the probabilistic assessment.
- The probabilistic WCS model shows a satisfactory fit to experimental data. Damage evolves from initial damage to unity at the rupture.
- The probabilistic assessment unveils the fact that WCS MCSR related material constants are more sensitive to the creep deformation behavior than SR related material constants.
- The probabilistic MCSR and SR bands subsist with the experimental bounds. The extrapolation capability of the probabilistic WCS framework tends to generate conservative prediction at the high temperature-low stress regimes.
- In this study, the calibration and variation of material constants are assumed to be independent of micro-structural damage and damage evolution. As creep is a complex deformation phenomenon for metallic materials and superalloys, such micro-structural degradation could potentially affect the fluctuation of material constants resulting in a variation of the model prediction.
- The probabilistic analysis should be based on the test data with sufficient population. However, creep test are normally very time consuming, and sometimes it is challenging to obtain sufficient data for accurate analysis. This may affect the industrial applicability of the probabilistic method in creep analysis. To address this issue Hossain et al. investigated the Accelerated Creep Test (ACT) to extract creep response of an alloy at ranges of temperature-stress from a single creep test [36].

Future probabilistic CDM-based WCS assessment will include the micro- and meso-scale degradation and component level simulation to enhance the degree of accuracy and predict high-fidelity creep-rupture estimates for newer candidate superalloys.

ACKNOWLEDGEMENTS

This material is based upon work supported by the Department of Energy National Energy Technology Laboratory under Award Number(s) DE-FE0027581.

This report was prepared as an account of work sponsored by an agency of the United States Government. Neither the United States Government nor any agency thereof, nor any of their employees, makes any warranty, express or implied, or assumes any legal liability or responsibility for the accuracy, completeness, or usefulness of any information, apparatus, product, or process disclosed, or represents that its use would not infringe privately owned rights. Reference herein to any specific commercial product, process, or service by trade name, trademark, manufacturer, or otherwise does not necessarily constitute or imply its endorsement, recommendation, or favoring by the United States Government or any agency thereof. The views and opinions of authors expressed herein do not necessarily state or reflect those of the United States Government or any agency thereof.

REFERENCES

[1] Vojdani, A., Farrahi, G. H., Mehmanparast, A., and Wang, B., 2018, "Probabilistic Assessment of Creep-Fatigue Crack Propagation in Austenitic Stainless Steel Cracked Plates," Eng. Fract. Mech., **200**(April), pp. 50–63.

[2] Davies, R. B., Hales, R., and Harman, J. C., 2016, "Statistical IVIodeling of Creep Rupture Data," 121(July 1999).

[3] Zentuti, N. A., Booker, J. D., Bradford, R. A. W., and Truman, C. E., 2018, "Correlations between Creep Parameters and Application to Probabilistic Damage Assessments," Int. J. Press. Vessel. Pip., **165**(July), pp. 295–305.

[4] Mao, H., and Mahadevan, S., 2000, "Reliability Analysis of Creep-Fatigue Failure," Int. J. Fatigue, **22**(9), pp. 789–797.

[5] Harlow, D. G., and Delph, T. J., 2000, "Creep Deformation and Failure: Effects of Randomness and Scatter," J. Eng. Mater. Technol. Trans. ASME, **122**(3), pp. 342–347.

[6] Rutman, W., Krause, M., and Kremer, K. J., 1966, "International Community Tests on Long-Term Behavior of 2-

1/4Cr-1Mo Steel." *Proc. Joint. Conf. on High-Temperature Properties of Steels*, Eastbourne, United Kingdom, British Iron and Steel Research Association and Iron and Steel Institute, pp. 232–239.
[7] Garofalo, F., Whitemore, R. W., Domis, W. F., and Vongemmingen, F., 1961, "Creep and Creep-Rupture Relationships in an Austenitic Stainless-Steel.," Trans. Metall. Soc. AIME, **221**(2), pp. 310–319.
[8] Penny, R. K., and Weber, M. A., 1992, "Robust Methods of Life Assessment during Creep," Int. J. Press. Vessel. Pip., **50**(1–3), pp. 109–131.
[9] Hayhurst, D. R., 1974, "The Effects of Test Variables on Scatter in High-Temperature Tensile Creep-Rupture Data," Int. J. Mech. Sci., **16**, pp. 829–841.
[10] Farris, J. P., Lee, J. D., Harlow, D. G., and Delph, T. J., 1990, "On the Scatter in Creep Rupture Times," Metall. Trans. A, **21**(1), pp. 345–352.
[11] Kim, S. J., Kong, Y. S., Roh, Y. J., and Kim, W. G., 2008, "Statistical Properties of Creep Rupture Data Distribution for STS304 Stainless Steels," Mater. Sci. Eng. A, **483**–**484**(1-2 C), pp. 529–532.
[12] Evans, M., 1994, "A Statistical Analysis of the Failure Time Distribution for 1/2Cr-1/2Mo- 1/4V Steel Tubes in the Presence of Outliers," Int. J. Press. Vessel. Pip., **60**(2), pp. 193–207.
[13] Booker, M. K., Booker, B. L. P., and Swindeman, R. W., 1982, "Analysis of Elevated-Temperature Tensile and Creep Properties of Normalized and Tempered 2.25Cr-1Mo Steel", Oak Ridge National Lab, TN (USA).
[14] Larson FR, Miller J. A time-dependence relationship for rupture and creep stresses. Trans ASME 1952;74:765–75.
[15] S.S. Manson, A.M. Haferd, "A Liner Time-Temperature Relation for Extrapolation of Creep and Stress-Rupture Data", National Advisory Committee for Aeronautics, Technical Notes 2890, March 1953.
[16] Appalanaidu, Y., Vyas, Y., and Gupta, S., 2013, "Stochastic Creep Damage Growth Due to Random Thermal Fluctuations Using Continuum Damage Mechanics," Procedia Eng., **55**, pp. 805–811.
[17] Kim, W. G., Park, J. Y., Hong, S. D., and Kim, S. J., 2011, "Probabilistic Assessment of Creep Crack Growth Rate for Gr. 91 Steel," Nucl. Eng. Des., **241**(9), pp. 3580–3586.
[18] Hossain, M. A., and Stewart, C. M., 2019, "Reliability Prediction of 304 Stainless Steel Using Sine-Hyperbolic Creep-Damage Model with Monte Carlo Simulation Method," *Proceedings of ASME 2019 Pressure Vessel and Piping Conference PVP2019*, San Antonio, Texas, USA.
[19] Zhao, J., Li, D. ming, Zhang, J. shan, Feng, W., and Fang, Y. yuan, 2009, "Introduction of SCRI Model for Creep Rupture Life Assessment," Int. J. Press. Vessel. Pip., **86**(9), pp. 599–603.
[20] Wilshire, B., and Scharning, P. J., 2007, "Long-Term Creep Life Prediction for a High Chromium Steel," Scr. Mater., **56**(8), pp. 701–704.
[21] Wilshire, B., Scharning, P. J., and Hurst, R., 2007, "New Methodology for Long Term Creep Data Generation for Power Plant Components," Energy Mater., **2**(2), pp. 84–88.
[22] Wilshire, B., and Scharning, P. J., 2008, "A New Methodology for Analysis of Creep and Creep Fracture Data for 9–12% Chromium Steels," Int. Mater. Rev., **53**(2), pp. 91–104.
[23] Wilshire, B., and Scharning, P. J., 2008, "Prediction of Long Term Creep Data for Forged 1Cr–1Mo–0·25V Steel," Mater. Sci. Technol., **24**(1), pp. 1–9.
[24] Cano, J. A., and Stewart, C. M., 2019, "Application of the Wilshire Stress-Rupture and Minimum-Creep-Strain-Rate Prediction Models for Alloys P91 in Tube, Plate, and Pipe Form," *Proceedings of ASME Turbo Expo 2019: Turbomachinery Technical Conference and Exposition GT2019*, Phoenix, Arizona, USA.
[25] Abdullah, Z., Perkins, K., and Williams, S., 2012, "Advances in the Wilshire Extrapolation Technique—Full Creep Curve Representation for the Aerospace Alloy Titanium 834," Mater. Sci. Eng. A, **550**, pp. 176–182.
[26] Whittaker, M. T., Evans, M., and Wilshire, B., 2012, "Long-Term Creep Data Prediction for Type 316H Stainless Steel.," Mater. Sci. Eng. A, **552**, pp. 145–150.
[27] Whittaker, M. T., and Harrison, W. J., 2014, "Evolution of Wilshire Equations for Creep Life Prediction," Mater. High Temp., **31**(3), pp. 233–238.
[28] Harrison, W. J., Whittaker, M. T., and Williams, S., 2013, "Recent Advances in Creep Modelling of the Nickel Base Superalloy, Alloy 720Li," Materials (Basel)., **6**(3), pp. 1118–1137.
[29] Evans, M., and Williams, T., 2019, "Assessing the Capability of the Wilshire Equations in Predicting Uniaxial Creep Curves: An Application to Waspaloy," Int. J. Press. Vessel. Pip., **172**, pp. 153–165.
[30] Stewart, C. M., 2013, "A Hybrid Constitutive Model for Creep, Fatigue, and Creep-Fatigue Damage," University of Central Florida.
[31] Hossain, M. A., and Stewart, C. M., 2020, "Probabilistic Minimum-Creep-Strain-Rate and Stress-Rupture Prediction for the Long-Term Assessment of IGT Components," *Proceedings of ASME Turbo Expo 2020: Turbomachinery Technical Conference and Exposition GT 2020*, London, England.
[32] Haque, M. S.; Stewart, C. M., 2016, "Modeling The Creep Deformation, Damage, and Rupture of Hastelloy X Using MPC Omega, Theta, and Sine-Hyperbolic Models.," *Proceedings of ASME 2016 Pressure Vessels and Piping Conference PVP 2016*, Vancouver, British Columbia, Canada, pp. 1–10.
[33] Haque, M. S., and Stewart, C. M., 2017, "The Stress-Sensitivity, Mesh-Dependence, and Convergence of Continuum Damage Mechanics Models for Creep," J. Press. Vessel Technol. Trans. ASME, **139**(4), pp. 1–10.
[34] American Society of Testing and Methods, 2015 "ASTM Standard E139 Test Method for Conducting Creep, Creep-Rupture, and Stress-Rupture Tests of Metallic Materials," ASTM International, West Conshohocken, PA.
[35] Standard Test Method for Tension Testing of Metallic Materials, August (2013), DOI: 10.1520/E0008_E0008M-13A.
[36] Hossain, M. A., Mach, R., Pellicotte, J., and Stewart, C. M., 2020, "Calibration of CDM-Based Creep Constitutive Model Using

Accelerated Creep Test (ACT) Data.," *Proceedings of ASME Turbo Expo 2020: Turbomachinery Technical Conference and Exposition GT 2020*, London, England.